

A NEW POTENTIAL FUNCTION FOR SELF INTERSECTING GIELIS CURVES WITH RATIONAL SYMMETRIES

Yohan D. Fougerolle, Frédéric Truchetet

LE2i Laboratory, UMR CNRS 5158, University of Burgundy, 12 rue de la fonderie, 71200 Le Creusot, France
yohan.fougerolle, frederic.truchetet@u-bourgogne.fr

Johan Gielis

Genicap Lab BV, Wilheminaeweg 1, 2042 NN, Zandvoort
johan@genicap.com

Keywords: Gielis curves and surfaces, implicit functions, parametric functions, R-functions, superquadrics, symmetry

Abstract: We present a new potential field equation for self-intersecting Gielis curves with rational rotational symmetries. In the literature, potential field equations for these curves, and their extensions to surfaces, impose the rotational symmetries to be integers in order to guarantee the unicity of the intersection between the curve/surface and any ray starting from its center. Although the representation with natural symmetries has been applied to mechanical parts modeling and reconstruction, the lack of a potential function for Rational symmetry Gielis Curves (RGC) remains a major problem for natural object representation, such as flowers and phyllotaxis. We overcome this problem by combining the potential values associated with the multiple intersections using R-functions. With this technique, several differentiable potential fields can be defined for RGCs. Especially, by performing N-ary R-conjunction or R-disjunction, two specific potential fields can be generated: one corresponding to the inner curve, that is the curve inscribed within the whole curve, and the outer -or envelope- that is the curve from which self intersections have been removed.

1 INTRODUCTION

Describing and modeling nature is fascinating and, generally speaking, one of the most fundamental research activities: whether to model physical behaviors or geometric structures, to describe or to recognize natural shapes, every research community aims at representing nature as accurately as possible. Classical models are largely based on isotropic spaces with the Euclidean circle as (isotropic) unit circle. In nature however, anisotropy is the rule and different ways of measuring or geometrizing exist. In 2003, halfway between the fields of botany and computer graphics, Gielis *et al.* introduced the superformula (Gielis, 2003; Gielis *et al.*, 2003), which can be seen as a parametric formulation for generalized circles or ellipses. Superellipses defining anisotropic unit circles led to notion of Minkowski distances and Minkowski geometry (Thompson, 1996). Superellipses have been extended to superquadrics in (Barr, 1981), which have found numerous applications due to the limited number of shape parameters and their ability to represent objects ranging from diamonds,

cubes, spheres, and any intermediate shape. More interestingly, the superformula is now spreading to other fields. For instance, it has been used in recent work to study constant mean curvature surfaces for anisotropic energies (Koiso and Palmer, 2008), in clustering and data mining in (Morales and Bobadilla, 2008), and in fluid dynamics in (Wang, 2008). Recently, Natalini *et al.* have presented a numerical algorithm to write down the explicit solution to the Dirichlet problem for the Laplace equation in a star-like domain (Natalini *et al.*, 2008), and presented closed form equations for various Gielis curves.

In 2005, based on the parametric formula proposed in (Gielis, 2003), potential fields for 3D Gielis surfaces have been proposed in (Fougerolle *et al.*, 2005). This representation has found applications for Gielis surface recovery for mechanical parts (Bokhabrine *et al.*, 2007). Unfortunately, one of its major weakness is that the implicit field equations require the rotational symmetries to be integers. Such a restriction can be tolerated when manufactured objects are represented. Unfortunately, as initially remarked in (Gielis, 2003), some natural objects

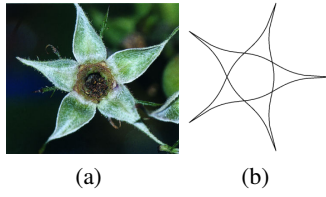


Figure 1: a) Rose sepals. b) RGC with $m = 5/2$ and $n_1 = n_2 = n_3 = 0.43$.

require the rotational symmetries to be rational numbers. Such symmetries are found in the phyllotaxy of plants. Leaves are arranged in a helical or spiral way around the stem. In rose, leaves are arranged around the stem in a $5/2$ arrangement, meaning that the sixth leaf will be precisely above the first one and the spacing between leaves is 144° . In wild roses the five petals are arranged in a plane, but the sepals in the preceding (almost planar) whorl still show the helical arrangement as they are still 144° apart. This arrangement can be seen using $m = 5/2$ in the superformula. It involves fusion of certain parts, while in the center an open structure is created, giving rise to the rose hip, as illustrated in Figure 1. Non-integer symmetries can be observed in biomolecules as well, *e.g.* DNA and proteins in which non-integer symmetries are observed frequently (Janner, 2001; Janner, 2005). Complex objects that are defined as Boolean operations between multiple globally deformed Gielis surfaces can be modeled and reconstructed (Fougerolle et al., 2005; Bokhbrine et al., 2007). To transcribe the Boolean predicates between 3D Gielis surfaces into analytical equations, R-functions have been employed. The strategy adopted in this paper uses the same tools and concepts, *i.e.* we use radial distance functions to build a 2D potential field, and R-functions for the transcription of Boolean combinations into analytical equations. The difference is that now we perform R-functions not to combine implicit fields of several Gielis curves or surfaces, but the multiple implicit values of the same rational Gielis curve. Thus, we overcome the self-intersection issue through an auto-R-function operation and build 2D potential fields equation for RGCs, that can represent for instance the envelope of the curve or its "core". We present several advantages of this representation, ranging from flower modeling, from global shape to petals, and its potential for further research directions, such as parameter recovery and/or optimization.

The structure of the rest of paper is as follows: in section 2 we recall the initial parametric definition of Gielis curves, surfaces, and their associated potential fields. In section 3 we briefly present R-functions. Using R-function and the initial Gielis formula, two

potential fields are presented for 2D RGCs in section 4. Several strategies about extension to Rational Gielis Surfaces are presented and discussed in section 5. We then present our future work and conclusions in section 6.

2 GIELIS CURVES

In polar coordinates, the radius $r(\theta)$ of a Gielis curve is defined by:

$$r(\phi) = \frac{1}{\sqrt[n_1]{\left|\frac{1}{a} \cos\left(\frac{m\phi}{4}\right)\right|^{n_2} + \left|\frac{1}{b} \sin\left(\frac{m\phi}{4}\right)\right|^{n_3}}}, \quad (1)$$

with $n_i \in \mathbb{R}^+$, and a, b , and $m \in \mathbb{R}_*^+$. Parameters a and b control the scale, m represents the number of rotational symmetries, n_1, n_2 , and n_3 are the shape coefficients. Regular polygons and superellipses can be generated by setting the shape coefficients to specific values as shown in (Gielis, 2003).

Gielis only proposed the parametric formulation for 2D curves. In the case of closed non self-intersecting curve (m is positive integer), for a 2D point $P(x, y)$ one can define the following potential field:

$$F_1(x, y) = 1 - \frac{\|\vec{OP}\|}{\|\vec{OI}\|} = 1 - \sqrt{\frac{x^2 + y^2}{r^2(\theta)}}. \quad (2)$$

O is the center of the curve, and the point $I = r(\theta(x, y))$ corresponds to the intersection between the curve and the half line $[OP)$. If the symmetry parameter m is an integer, the intersection I is unique. If the curve is closed, the sign of the potential field $F(x, y)$ generated by equation 2 can be used to define a partition of the 2D space. In this case, the set of points where $F(x, y)$ is positive corresponds to the inside of the Gielis curve, the set of points where $F(x, y)$ is negative corresponds to its outside, and the curve corresponds to the zero-set of the potential field.

In (Fougerolle et al., 2005), by setting $a = b = 1$ in equation 1 and by considering a 3D Gielis surface as the spherical product of two 2D Gielis curves, potential fields for 3D non self-intersecting Gielis surfaces have been introduced as:

$$F_2(x, y, z) = 1 - \frac{1}{r_2(\phi)} \sqrt{\frac{x^2 + y^2 + z^2}{\cos^2 \phi (r_1^2(\theta) - 1) + 1}}. \quad (3)$$

Such representation of Gielis surfaces as iso-values of a potential field is crucial for Gielis surface reconstruction from 3D data, because it is used to build various cost functions to be optimized.

3 R-FUNCTIONS

R-functions find their origin in geometric algebra based on logic and have been introduced by Vladimir Logvinovich Rvachev in (Rvachev, 1967). Since their introduction, R-functions have found direct applications in several fields, such as geometric modeling and boundary value problems. For conciseness purpose, we briefly present the most common R-functions in this section. The reader is invited to refer to the recent survey by Shapiro (Shapiro, 2007) for more in depth presentation of R-functions and their applications.

The simplest R-function is $R_\alpha(x_1, x_2)$ and is defined by:

$$R_\alpha(x_1, x_2) = \frac{1}{1+\alpha} \left(x_1 + x_2 \pm \sqrt{x_1^2 + x_2^2 - 2\alpha x_1 x_2} \right), \quad (4)$$

where $\alpha(x_1, x_2)$ is an arbitrary symmetric function such that $-1 < \alpha(x_1, x_2) \leq 1$. Setting α to 1 leads to the simplest and most popular R-functions: R-conjunction $\min(x_1, x_2)$ and R-disjunction $\max(x_1, x_2)$. Other useful R-functions with differential and normalization properties, namely R_0^m and R_p , are studied in detail in (Shapiro and Tsukanov, 1999), and are respectively defined by:

$$R_0^m(x_1, x_2) = \left(x_1 + x_2 \pm \sqrt{x_1^2 + x_2^2} \right) (x_1^2 + x_2^2)^{\frac{m}{2}}, \quad (5)$$

where m is any even positive integer and

$$R_p(x_1, x_2) = x_1 + x_2 \pm (x_1^p + x_2^p)^{\frac{1}{p}}, \quad (6)$$

for any even positive integer p . R_α , R_0^m , and R_p functions only handle two arguments. Rvachev introduced the N -ary R-conjunction and R-disjunction to handle more than two arguments, which are less restrictive than R_α , R_0^m , and R_p and more appropriate to RGCs. The parameter m is an integer and corresponds to the parameter used for R_m functions.

$$\bigwedge_{i=1}^{i=n(m)} x_i \equiv \sum_{i=1}^n (-1)^m x_i^m (x_i - |x_i|) + \prod_{i=1}^n x_i^m (x_i + |x_i|). \quad (7a)$$

$$\bigvee_{i=1}^{i=n(m)} x_i \equiv \sum_{i=1}^n x_i^m (x_i + |x_i|) - \prod_{i=1}^n x_i^m (-1)^m (|x_i| - x_i). \quad (7b)$$

If no specific constraint about differentiability is required, m can be set to zero, which leads to the simplified version of N -ary R-conjunction and R-disjunction defined in equations 8a and 8b.

$$\bigwedge_{i=1}^{i=n} x_i \equiv \sum_{i=1}^n (x_i - |x_i|) + \prod_{i=1}^n (x_i + |x_i|). \quad (8a)$$

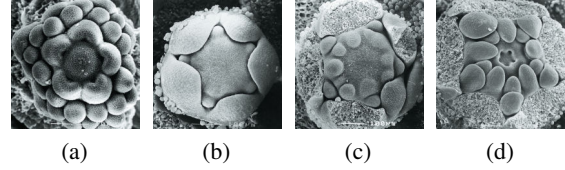


Figure 2: Examples of developing flower buds. a) *Ochna atropurpurea*: Development of ovary. b) *Greyia sutherlandii* stage 1: sepals protect the newly formed petals. c) *Greyia sutherlandii* stage 2: stamens develop with petals in the five corners of the pentagon (sepals removed). d) *Greyia sutherlandii* stage 3: stamens and pistils develop.

$$\bigvee_{i=1}^{i=n} x_i \equiv \sum_{i=1}^n (x_i + |x_i|) - \prod_{i=1}^n (|x_i| - x_i). \quad (8b)$$

An R-function is a real-valued function characterized by some property that is completely determined by the corresponding property of its arguments. More specifically, the R-functions presented in this paper have the property that their sign is completely determined by the signs of their arguments. In the following section, we present how to use this property to build a signed potential field for RGCs.

4 POTENTIAL FIELD EQUATION FOR RATIONAL GIELIS CURVES

While RGC curves with multiple crossings and period k (with k even) can be studied in a XY graph without intersections, it is worthwhile to develop a potential field function which does take the intersections into account and in which multiple function values do occur. As observed in rose, such intersections could indeed give rise to a center which can develop into the rose hip. Alternatively, the multiple intersections can lead to the separation of specific, isolated sectors in which separate developmental processes may occur. Such sectors are indeed observed using R-conjunction of outer envelope and the complementary of the core (Figure 5). At the bud stage, flower development involves the sequential initiation of various whorls in well-defined yet separated sectors. In *Greyia sutherlandii* (Figures 2(b), 2(c), and 2(d)) for example, after the formation of sepals in the 'corners' petals are formed and inbetween the formation of stamens occurs.

We come back to the superformula initial formulation and introduce rational symmetry: the symmetry parameter m is no longer an integer and can be rational, and $a = b = 1$. By definition, RGCs are self inter-

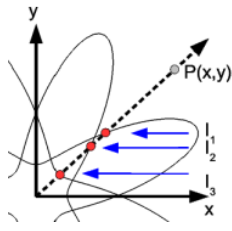


Figure 3: Intersections between a RGC with $m = 8/3$ and a half ray.

secting curves, *i.e.* the symmetry parameter m can be written as the ratio of two integers as $m = p/q$. The parametric formulation of a RGC is then written as:

$$r(\phi) = \frac{1}{\sqrt[n_1]{\left|\cos\left(\frac{p\phi}{4q}\right)\right|^{n_2} + \left|\sin\left(\frac{p\phi}{4q}\right)\right|^{n_3}}}, \quad (9)$$

with $p, q \in \mathbb{N}_*^+$. The parameter p is similar to m , *i.e.* still represents the rotational symmetry number. The parameter q corresponds to the maximum number of self intersections, and the angle θ now belongs to $[0, 2q\pi]$. The condition for a RGC to be closed is to verify that the radius $r(\theta)$ is identical for angles $\theta = 0$ and $\theta = 2q\pi$, which can be written as $r(0) = r(2q\pi)$.

Figure 3 shows an example of a RGC with $p = 8$ and $q = 3$. For a given RGC, there exist multiple intersections between a ray originated from its center and the curve, *i.e.* there exist multiple polar coordinates in $[0, 2q\pi]$ that generate points lying both on the curve and the ray, as illustrated in Figure 3, where three intersections, noted I_1, I_2 and I_3 are detected. The number of intersections depends on q and double intersection points appear for angles $\theta = kp/q$. For a given point $P(x, y)$, a first angle θ_0 within $[0, 2\pi]$ can be easily determined. The corresponding intersection point I_0 can be computed as $r(\theta_0)$. Other angles θ_k and corresponding intersection points I_k can easily be determined using $\theta_k = \theta_0 + 2k\pi$ and $I_k = r(\theta_k)$. We see that the several intersections can be simply computed and correspond to the multiple values of the radius for $\theta_0 + 2k\pi$ values. For each intersection point I_k , equation 2 can be applied to associate a potential.

Now, the last problem to overcome is to build a continuous potential field from these k individual potentials. One of the simplest idea is to consider the maximum or minimum potential determined for intersection points I_k using equation 4 with $\alpha = 1$. This approach generates a potential field that is not smooth everywhere, as illustrated in Figures 4(b), 4(d), 4(f), 4(h), ??, and ??, that have been obtained using min and max R-functions. Therefore, such a technique suffers a severe drawback, especially for reconstruction purposes, where differentiable functions are often

preferred. To obtain a differentiable potential field, we can combine each potential using R-functions presented in equations 5 or 6. Using R_p may be an advantage if normalization property is desired, but it also has a major drawback. With R_p -functions, the generated potential field depends on the order the R-functions. Indeed, for instance, it is easy to verify that $(x_1 \wedge x_2) \wedge x_3 \neq x_1 \wedge (x_2 \wedge x_3)$, except over its zero-set. Unicity of the potential field can be obtained using two techniques: sort individual values or restrict the q parameter to be set to 2 to keep binary R-functions, which is not satisfactory in both cases. Fortunately, for multiple self intersections, n potential values can be combined using n -ary R-functions as defined in equation 7. The justification for the introduction of equations 8a and 8b now clearly appears: using binary R-functions, such as R_α , R_p or R_m , restricts the parameter q in equation 9 to be equal to 2, whereas with N-ary R-functions $q \in \mathbb{N}_*^+$. The commutativity of N-ary R-functions is obvious since these functions are a sum of sums and products that are commutative.

Eventually, by replacing the arguments of equations 8a and 8b by the potential field defined in equation 2, we obtain the inner and outer potential fields for 2D-RGCs, respectively defined by:

$$\bigwedge_{i=1}^{i=q} F_1(x_i, y_i) \text{ and } \bigvee_{i=1}^{i=q} F_1(x_i, y_i), \quad (10)$$

where $F_1(x_i, y_i)$ corresponds to the potentials evaluated for the multiple intersection points (x_i, y_i) using equation 2 combined through N-ary R-conjunction and R-disjunction, respectively. Figure 4 illustrates the relative intensity of the potential field for various RGCs and several R-functions.

Additionally, the inner and outer potential fields can be combined together, for example to represent developmental processes in flowers. For instance, one can want to perform the equivalent of the Boolean difference between the inner and outer curve, simply by using binary R-functions, as illustrated in Figure 5. Such a representation finds direct biological meaning: when a plant goes into flowering, the flower approximately becomes a planar structure, going from a spiral phyllotaxy (given by Fibonacci numbers) into a planar phyllotaxy or still with helical or spiral tendencies. But in a meristem of the flower, new entities have to develop sequentially (first sepals, followed by petals, stamen and finally pistil). This means that in a planar arrangement a clear separation of areas/sectors is necessary, as delineation of potential fields. And that is precisely what distinguishes Figures 4 and 5. This illustrates the potential of our approach to build from bottom up (pure R-functions/logic, with RGC) a way of modeling flowers. This example also illustrates the

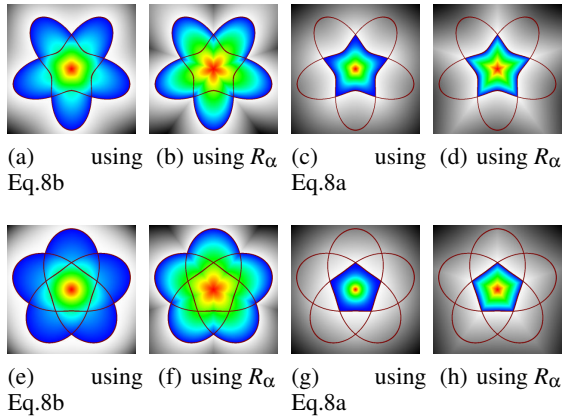


Figure 4: Color coding of relative intensity of the potential field generated by auto R-function of a RGC with $a = b = 1$, $n_1 = 0.5$, $n_2 = n_3 = 3.5$, $p = 5$. The RGC is in dark red. First row: $m = 5/2$. Second row $m = 5/3$. From left to right: relative potential field intensity using the N-ary R-disjunction, Maximum, N-ary R-conjunction, and Minimum.

strength of our approach, thanks to R-functions, because such sectors may not be represented using Natalini's approach.

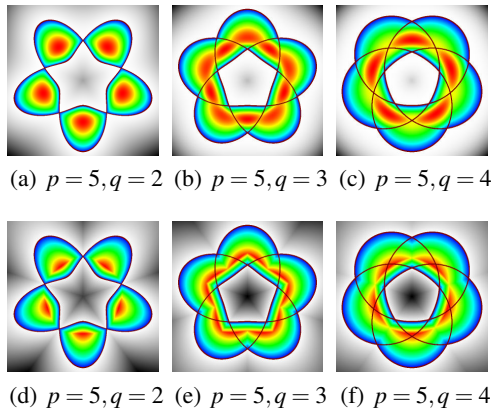


Figure 5: R-conjunction between a RGC outer envelope and the complementary of its inner envelope to represent various petal shapes. First row: using R_p -function. Second row: using R_α .

5 EXTENSION TO RATIONAL GIELIS SURFACES

We present two approaches to extend RGCs to Rational Gielis Surfaces (RGSs). The first one is using spherical product, and the second is building revolution surfaces using a RGC and a profile. The ob-

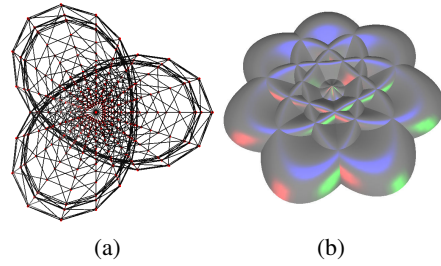


Figure 6: Rational Gielis Surfaces. a) Spherical product. b) Revolution surface.

jective of 3D extension through spherical product is to generate a closed surface built upon two Gielis curves, which can be used in solid modeling for example. This operation requires one important restriction: the second generating curve cannot be rational. The main problems arising when considering a RGC as second generating curve are surface generation/continuity and potential field evaluation. In spherical product, half of the second curve, that corresponds to angles $\phi \in [-\frac{\pi}{2}, \frac{\pi}{2}]$, is rotated around the rotation axis of the first generating curve. In this case, the $2q\pi$ modulus to evaluate every intersection leads to curve discontinuities, which is a major problem for efficient and simple tessellation algorithms and potential field evaluation. Thus, one solution to build closed surfaces while preserving surface continuity and signed implicit field definition, is to perform the spherical product between one RGC with one GC. The implicit field generated can then be evaluated by:

$$\bigwedge_{i=1}^{i=q} F_2(x_i, y_i) \text{ and } \bigvee_{i=1}^{i=q} F_2(x_i, y_i), \quad (11)$$

where $F_2(x, y)$ is the potential equation for 3D Gielis Surfaces presented in equation 3. An example of a mesh corresponding to such surface is illustrated in Figure 6(a).

The second approach consists in defining a profile, by any known techniques such as NURBS for instance, and to use this profile as an elevation profile. In this case, the surface created does not define a closed object, which makes impossible the expression of an implicit field. Nevertheless, such representation may be very useful for compact and efficient representation of elementary 3D flower patterns, especially in entertainment or video-game industry. An example of a revolution surface using RGC, using a cubic polynomial profile, is presented in 6(b).

6 CONCLUSIONS

We have presented new potential functions for closed Rational Gielis Curves and possible strategies for their extension to 3D surfaces. Our approach makes use of R-functions to overcome the self-intersections issue introduced by the rational rotational symmetry. With this technique, several differentiable potential fields can be defined for RGCs and, more specifically, one corresponding to the inner curve, that is the curve inscribed within the whole curve, and one corresponding to the envelope. Such representation offers promising perspectives, especially in botany with classification and morphology metrics: as illustrated in Figure 5, combining inner and outer potential fields through R-functions leads to the definition of sectors that are directly related to the flower developmental process.

Among the numerous other research directions, we consider the study of other possible 3D extensions and their applications to solid modeling, boundary value problems, and/or entertainment (fast 3D flower modeling and rendering, procedural flower field texture generation, etc). Another still highly challenging research concerns the shape and symmetry parameters recovery. To our knowledge, in the literature, there still exist very few papers dedicated to Gielis curves parameters recovery using integer symmetries, and none considering rational symmetries. The introduction of potential equations for such closed curves therefore opens new research perspectives in this field. Moreover, due to the complexity of the space parameters, deterministic methods, such as Levenberg-Marquardt method, can only be applied in restricted cases, with prior symmetry detections and strong assumptions. Our current and future works include the development of more suitable RGC potential functions for optimization processes combined with the study of appropriate stochastic algorithms for efficient RGCs parameters recovery and their application to classification, pattern recognition, and object segmentation both in 2D and 3D.

REFERENCES

- Barr, A. H. (1981). Superquadrics and angle-preserving transformations. *IEEE Computer Graphics and Applications*, 1(1):481–484.
- Berger, M. (2000). Encounter with a geometer. *Notices of the American Mathematical Society*, 47(2.1, 3.2).
- Bokhabrine, Y., Fougerolle, Y. D., Fougou, S., and Truchetet, F. (2007). Genetic algorithms for Gielis surface recovery from 3D data sets. In *Proceedings of the International Conference on Image Processing ICIP'07*, pages 549–542, San Antonio, TX, USA.
- Fougerolle, Y. D., Gribok, A., Fougou, S., Truchetet, F., and Abidi, M. A. (2005). Boolean operations with implicit and parametric representation of primitives using R-functions. *IEEE Transactions on Visualisation and Computer Graphics*, 11(5):529–539.
- Fougerolle, Y. D., Gribok, A., Fougou, S., Truchetet, F., and Abidi, M. A. (2006). Supershape recovery from 3D data sets. In *Proceedings of the International Conference on Image Processing ICIP'06*, pages 2193–2196, Atlanta, GA, USA.
- Gielis, J. (2003). A generic geometric transformation that unifies a wide range of natural and abstract shapes. *American Journal of Botany*, 90:333–338.
- Gielis, J., Beirinckx, B., and Bastiaens, E. (2003). Superquadrics with rational and irrational symmetry. In Elber, G. and Shapiro, V., editors, *Proceedings of the 8th ACM Symposium on Solid Modeling and Applications*, pages 262–265, Seattle.
- Janner, A. (2001). DNA enclosing forms from scaled growth forms of snow crystals. *Crystal Engineering*, 4(2-3):119–129.
- Janner, A. (2005). Strongly correlated structure of axial-symmetric proteins. ii. pentagonal, heptagonal, octagonal, nonagonal and ondecagonal symmetries. *Acta Crystallogr, section D, Biological Crystallography*, 61(3):256–68.
- Koiso, M. and Palmer, B. (2008). Equilibria for anisotropic surface energies and the Gielis formula. *Forma (Japanese Society on Form, accepted for publication)*, N.A.(N.A.).
- Morales, A. K. and Bobadilla, E. (2008). Clustering with an n-dimensional extension of Gielis superformula. In *Proceedings of 7th WSEAS Int. Conf. on ARTIFICIAL INTELLIGENCE, KNOWLEDGE ENGINEERING and DATA BASES (AIKED'08)*, University of Cambridge, UK.
- Natalini, P., Patrizi, R., and Ricci, E. (2008). The Dirichlet problem for the Laplace equation in a starlike domain of a Riemann surface. *Numerical Algorithms*, N.A. available online at www.springer.com.
- Rvachev, V. L. (1967). *Geometric Applications of Logic Algebra*. Naukova Dumka. In Russian.
- Shapiro, V. (2007). Semi analytic geometry with R-functions. *ACTA Numerica*, 16:239–303.
- Shapiro, V. and Tsukanov, I. (1999). Implicit functions with guaranteed differential properties. In *Symposium on Solid Modeling and Applications*, pages 258–269.
- Thompson, A. (1996). *Minkowski geometry*, volume 63 of *Encyclopedia of Mathematics and its applications*. Cambridge University Press.
- Wang, H. (2008). Investigation of trajectories of inviscid fluid particles in two-dimensional rotating boxes. *Theoretical Computational Fluid Dynamics*, 22:21–35.